

# A Scattering Wavelet Network-based Approach to Fingerprint Classification

Parmeshwar Birajadar<sup>1</sup>, Vikram Gadre<sup>2</sup>

<sup>1</sup>Department of Electronics Engineering, VESIT, Mumbai University, Mumbai, India 400 071

<sup>2</sup>Department of Electrical Engineering, IIT Bombay, Mumbai, India 400 076

## ABSTRACT

In a large-scale automatic fingerprint identification system (AFIS), fingerprint classification is an essential indexing step to reduce the search time in a large database for accurate matching. Fingerprint classification is still a challenging machine learning problem due to large intra-class and small inter-class variability. Nonlinear elastic deformation is one of the main sources of intra-class variability, which occurs due to the non-uniform pressure applied during fingerprint acquisition and the elastic nature of the fingerprint itself. This paper proposes a novel approach to fingerprint classification based on a scattering wavelet network to extract translation and small deformation invariant local features. The resulting sparse invariant feature vectors are used as input to a simple generative PCA affine classifier for the classification. The experiments evaluated with two different protocols on a benchmark NIST SD-4 database show the effectiveness and robustness of the proposed fingerprint classification algorithm in terms of classification accuracy.

**Keywords:** Biometrics, Fingerprint classification, PCA affine classifier, Scattering wavelet network.

*SAMRIDDHI : A Journal of Physical Sciences, Engineering and Technology* (2022); DOI: 10.18090/samriddhi.v14i02.1

## INTRODUCTION

Fingerprint indexing is becoming increasingly important due to the widespread use of fingerprints as a biometric trait in commercial, healthcare, and criminal identification. Fingerprint classification is commonly used for the initial coarse classification of the database into different classes to reduce the search space and is very useful in ten-print matching applications.

Continuous classification<sup>[1]</sup> and exclusive (fixed) classification<sup>[2]</sup> are the two main approaches used in most automatic fingerprint identification systems (AFIS). In the case of continuous classification, a large database is partitioned into different classes (clusters) having similar features, whereas, in exclusive classification, it is divided into fixed predefined classes. Most of the classification algorithms, including ours, use the human interpretable Galton-Henry classification<sup>[3]</sup> system, in which fingerprints are classified into five classes, namely Right loop (R), Left loop (L), Arch (A), Tented Arch (T) and Whorl (W) as shown in Figure 1. The

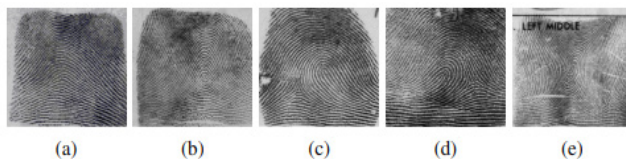


**Figure 1:** Five major classes of fingerprint: a) Arch, b) Tented Arch, c) Right loop, d) Left loop, e) Whorl.

**Corresponding Author:** Parmeshwar Birajadar, Department of Electronics Engineering, VESIT, Mumbai University, Mumbai, India 400 071, e-mail: parmeshwar.birajadar@ves.ac.in

**How to cite this article:** Birajadar, P., Gadre, V. (2022). A Scattering Wavelet Network-based Approach to Fingerprint Classification. *SAMRIDDHI : A Journal of Physical Sciences, Engineering and Technology*, 14(2), 130-138.

**Source of support:** Nil

**Conflict of interest:** None

natural distribution of these classes is 31.7%, 33.8%, 3.7%, 2.9% and 27.9%, respectively. Fingerprint classification is still a challenging machine learning problem<sup>[4]</sup> due to large intra-class and small inter-class variability and inherent background noise.

Many methods to address this problem have been proposed in the literature and commonly used approaches can be broadly classified as Rule-based,<sup>[2,5,6]</sup> Syntactic,<sup>[7]</sup> Structural,<sup>[8]</sup> Neural Network,<sup>[9-11]</sup> SVM Support

Vector Machine),<sup>[12-14]</sup> k-Nearest Neighbor (k-NN)<sup>[10,14]</sup> and Hybrid (Multi-Classifer).<sup>[9,10,13,14]</sup> Comprehensive reviews of fingerprint classification techniques have been proposed.<sup>[15,16]</sup> Galar *et al.*<sup>[15]</sup> have presented a critical review of all the existing methods for fingerprint classification highlighting their relative merits and demerits,<sup>[16]</sup> they have put forward a common testing platform and a comparative analysis by implementing commonly used algorithms for fingerprint

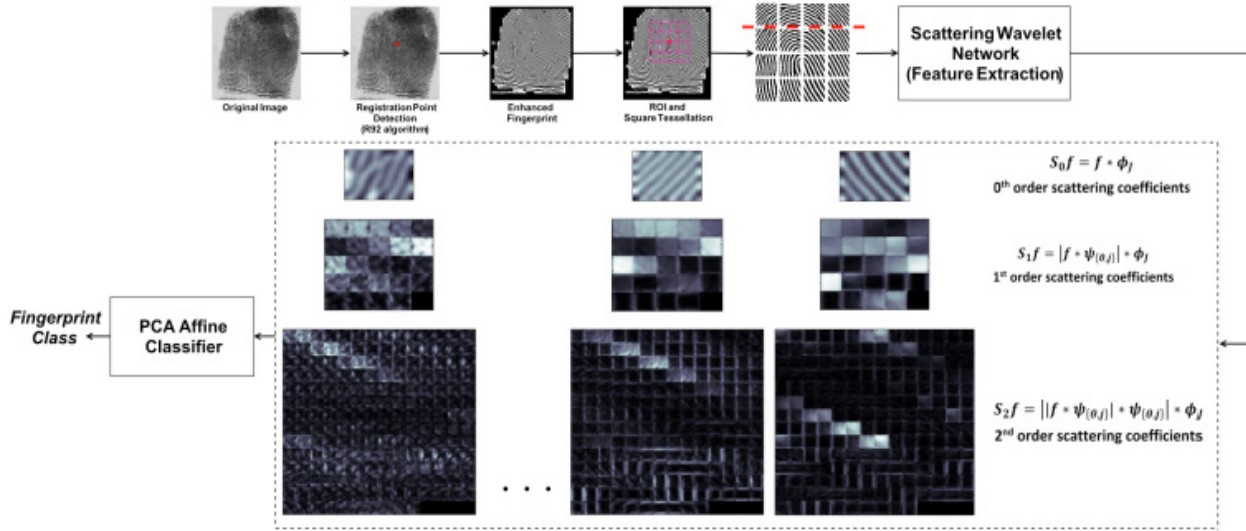


**Figure 2:** Flowchart of the proposed scattering wavelet network based fingerprint classification approach. The top row shows the preprocessing steps of ROI extraction. The blocks above the red dashed line are not included for feature extraction. The bottom dashed rectangle shows the sparse scattering wavelet decomposition of 3 different blocks from the ROI.

classification. Hence, we have followed the guidelines and the performance evaluation protocol for the NIST SD-4 database suggested by Galar *et al.*<sup>[16]</sup> to evaluate our algorithm in section 5 of the paper. Different types of fingerprint features have been utilized for fingerprint classification such as singular points,<sup>[2,5,6]</sup> orientation field,<sup>[8,9]</sup> ridge structure,<sup>[9,13]</sup> oriented texture information by means of filter responses.<sup>[10,13]</sup> Many attempts in the literature also use a combination of these features<sup>[9,10,13,14]</sup> to increase classification accuracy. Out of these, the level-1 features (singular points and orientation field) are the most popular. Recent deep learning approaches<sup>[17-19]</sup> are also proposed in the literature for fingerprint classification. The standard NIST SD-4 fingerprint database is commonly used as a benchmark in almost all the fingerprint classification research work. Hence, we use the same database for the performance evaluation of the proposed algorithm.

In live-scan and noisy fingerprints, the detection of singular points is difficult, so the methods based on filter responses outperform<sup>[16]</sup> the methods based on level-1 features. Nonlinear elastic deformation is one of the main sources of intra-class variability (variations among different fingerprint samples from the same finger), which occurs due to the non-uniform pressure applied during fingerprint acquisition and the elastic nature of the fingerprint itself. Gabor filter-based features<sup>[10]</sup> are widely used in texture-based fingerprint classification, but invariance to deformation is not considered.

This work proposes a novel approach to fingerprint classification based on a scattering wavelet network<sup>[20]</sup> for translation and small deformation invariant local texture

feature extraction. The block diagram of our classification scheme is shown in Figure 2. It consists of the following main steps :

- Determine the registration point using the R92 algorithm<sup>[21]</sup> and perform fingerprint enhancement.
- Crop the region of interest (ROI) around the registration point and perform a square tessellation of ROI.
- Apply second-order scattering wavelet transform using oriented Morlet wavelet filterbank on each local block.
- Calculate the mean of the scattering coefficients for each block of the ROI and obtain the final feature vector by concatenating the mean feature for all the blocks.
- Feed the feature vector to a trained PCA (Principal Component Analysis) affine classifier to perform fingerprint classification.

The rest of this paper is organized as follows. Section 2 introduces a scattering wavelet network architecture and its importance to texture classification. In section 3, we describe the details of the feature extraction process of the proposed classification algorithm. This is followed by section 4, which describes the PCA-based classification. In section 5, experimental results are summarized using two different protocols on the NIST SD-4 database. Section 6 then concludes the paper.

## SCATTERING WAVELET NETWORK

With the spirit of deep convolution networks, Mallat<sup>[22,23]</sup> introduced the Scattering Wavelet Network (ScatNet) using a cascade of the wavelet transform and a modulus operator as shown in Figure 3 build representations of signals.

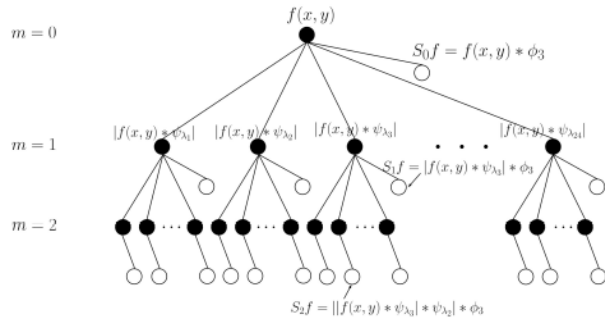


**Figure 3:** Scattering Wavelet Network for orders  $m = 0, 1, 2$  with three scales ( $J = 3$ ) and eight orientations ( $L = 8$ ). Hence,  $\lambda = (\theta, j)$  varies from  $\lambda_1$  to  $\lambda_{24}$ . White and black circles represent the scattering coefficients and wavelet modulus, respectively.



**Figure 4:** Two impressions of the same finger: (a) F0026, (b) S0026.

### Architecture of SCATNETS

Let the input image be denoted as  $f(v)$ , where  $v \in \mathbb{R}^2$ . To build a scattering wavelet transform, let  $\phi_j(v) = 2^{-2j}\phi(2^{-j}v)$  be a Gaussian lowpass filter controlled by scaling factor  $J$ .  $\psi$  is the mother wavelet, whose dilated and rotated versions are denoted by  $\{\psi_\lambda\}$  where  $\lambda = (\theta, j)$ ,  $\theta$  is the orientation and  $2^j$  are the dyadic scales, where  $j \in \{1, 2, \dots, J\}$ .

The calculation of the scattering coefficients of each layer is pictorially represented in Figure 3. The theoretical and implementation details of the scattering wavelet network can be found on the webpage (<http://www.di.ens.fr/data/scattering/>) and references given therein.

### ScatNet and fingerprint classification

Since fingerprints have quasi-periodic ridge-valley texture information, several researchers<sup>[10,13]</sup> utilize the texture information for fingerprint recognition and classification. Even though Scatnet has successfully classified other textural databases, in the case of fingerprint classification, building an invariant representation using Scatnet is a challenging task because the useful classification information (oriented texture) is located in different regions of the fingerprint with small intraclass variability. Hence, we preferred the block-based approach for local feature extraction. Along with the common sources of variability such as translation and

rotation, deformation is another crucial source of variability. Figure 4 shows two impressions of the same finger from the NIST SD-4 database. The non-linear deformation is clearly seen between the two impressions of the same finger. Dividing the ROI into 16 blocks linearizes the deformation to some extent, but Scatnet features are extracted for each of these blocks to build a complete local deformation invariant model. Thus, the blockwise Scatnet approach is useful in two ways. First, the oriental ridge-furrow structural information gets divided into local blocks and second, a small deformation present in respective blocks can easily be linearized by means of scattering features.

### FEATURE EXTRACTION

The fingerprint class is generally decided by its global ridge valley structural information. So the effective capture of this information in a feature vector is most important. This work constructs a fixed-size feature vector from the multilayer scattering coefficients for fingerprint classification.

Firstly, we locate the reference point in the fingerprint and a fixed size square ROI is cropped around this point. Secondly, the ROI is enhanced using a Gabor filterbank-based method. Thirdly, a square tessellation of the enhanced ROI is performed into different blocks. Finally, a third-order scattering wavelet transform is applied on each block to form a feature vector.

### Registration Point Detection and Enhancement

In order to determine the region of interest (ROI), a reference point is located and an area of size  $220 \times 220$  is cropped around it to extract the most dominant features for classification. Locating the reference point accurately is crucial to extracting similar features of intraclass fingerprints. Generally, the point where the maximum orientation change occurs is considered as a reference or registration point. Many reference point detection methods<sup>[2,10]</sup> have been proposed in the literature for fingerprint alignment during matching and classification. In many cases, the core point itself is considered the reference point, but this method is not preferred since arch-type fingerprints have no core point. The widely used rule-based R92 algorithm<sup>[21]</sup> is used for reference point detection in this work. The R92 algorithm consistently detects a point with the largest orientation variance as the registration point for all types of fingerprints including the arch type. The C-routines of the R92 algorithm in the open-source NIST Biometric Image Software (NBIS)<sup>[24]</sup> are used to detect the reference point.

The robustness of the feature extraction and classification performance can be increased<sup>[11]</sup> by introducing an enhancement stage prior to feature extraction. The widely used algorithm proposed by Hong *et al.*<sup>[25]</sup> is used for the enhancement of cropped ROI. The enhancement algorithm consists of four stages namely: *Normalization, Local Orientation estimation, Local frequency estimation, and Gabor filtering.*



### ScatNet Parameters and Feature Vector Construction

In general, any real or complex wavelet can be used to build a scattering wavelet framework, but **oriented** complex wavelets have been used to capture directional information in fingerprints. Since fingerprints are quasi-periodic in nature, a complex wavelet is better adapted for capturing the oscillatory behavior of fingerprints. The most obvious choice is the Gabor wavelets used in many image processing applications due to the best joint spatial and frequency localization. Since the Gabor wavelet has a non-zero mean which makes the feature vectors non-sparse. Hence, a variant of the Gabor wavelet called the Morlet wavelet is used for classification. For angular sensitivity, the circular envelope of the wavelet is replaced with an elliptical one by introducing a parameter for eccentricity ( $\epsilon$ ) as:

$$\psi_{Morlet}(x, y) = \frac{\epsilon}{2\pi\sigma^2} \exp\left(\frac{-(x^2 + \epsilon^2 y^2)}{2\sigma^2}\right) (\exp(i\omega x) - \beta) \quad (1)$$

where the constant  $\beta$  is selected so that its mean becomes zero. We have used a Morlet wavelet, as shown in Figure 5, with parameters  $\omega = 3\pi/4$ ,  $\epsilon = 0.5$  and  $\sigma = 0.8$  in all the classification experiments. Generally, in 500 dpi resolution fingerprint images, inter-ridge spacing is up to 10 pixels,<sup>[10]</sup> hence the first scale frequency of Morlet wavelet is set as  $\omega = 3\pi/4$ . The choice of  $\sigma = 0.8$  is a trade-off between a zero mean wavelet condition and Littlewood-Paley sum for the scattering wavelet filter bank [20] and hence is set to 0.8 with  $\omega = 3\pi/4$ . For a better angular and scale sensitivity, the eccentricity parameter  $\epsilon$  is selected as  $\epsilon = 4/L$  and is 0.5 with the chosen  $L = 8$  orientations. The family of multi-scale oriented wavelets is constructed from the above wavelet as:

$$\psi_{\theta,j}(v) = 2^{-2j} \psi(2^{-j} R_{\theta} v) \quad (2)$$

where  $v = (x, y)$  and  $R_{\theta}$  is the rotation matrix with  $\theta = [0, 2\pi)$ . We have selected the number of scales  $J = 3$  and orientations  $L = 8$  to build the fingerprint scattering features using Morlet wavelets as described in section 2. For feature extraction, the ROI of size  $220 \times 220$  is divided into 16 blocks of size  $55 \times 55$ .

The top 4 blocks (the blocks above the dotted red line as shown in Figure 2) are not used for feature extraction because the most discriminative information is present in the lower part of the fingerprint. A three-layer (order  $m = 2$ ) scattering wavelet transform is applied on each block. The

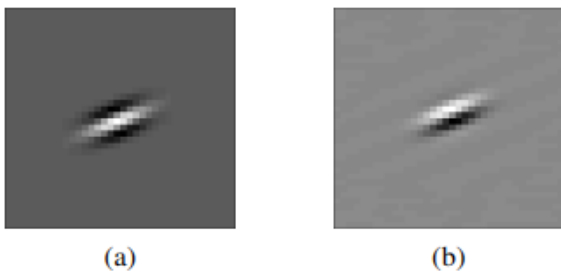


**Figure 5:** Morlet wavelet ( $\psi$ ): (a) Real part, (b) Imaginary part.

size of the scattering vector of the  $p$ -th layer is given by  $J_p$ . We then calculate the mean of each transformed block. The final feature vector (FV) is obtained by concatenating the feature vectors of all the 12 blocks as:

$$FV = (FV_{b1}, FV_{b2}, FV_{b3}, \dots, FV_{b12}) \quad (3)$$

The final feature vector length is given by

$$12 \times \sum_{p=0}^m L^p \binom{J}{P} \quad (4)$$

which equals 2604 with the selected parameters: ( $m = 2, J = 3, L = 8$ ).

### PCA AFFINE CLASSIFIER

PCA was originally devised for dimensionality reduction, but due to its capability of extracting the principal components of a dataset, PCA has found extensive applications in the field of classification. The PCA-based classifier is a supervised generative model. During the training, an affine space is created for each class. After generating the model, test vector is projected onto each of these spaces, and the best fitting space is chosen as the assigned class. The first step is to create the covariance matrix. The principal components correspond to the eigenvectors of the covariance matrix. Since the matrix is symmetric, the obtained components are orthogonal. The affine coordinate space is created by taking  $K$  principal components with the largest eigenvalues. The test vector is projected into each of the class spaces:

$$Y' = Y P_K \quad (5)$$

where the columns of  $P_K$  are the  $K$  principal components and the assigned label is defined as:

$$\underset{c=1, \dots, n}{\operatorname{argmin}} \|Y'_c - Y\| \quad (6)$$

where  $n$  is the number of classes and  $Y'_c$  is the projection of  $Y$  for class  $c$ . Bruna *et al.*<sup>[20]</sup> showed that the PCA-based generative model classifier outperforms SVM for smaller datasets, specifically for scattering features.

### EXPERIMENTAL RESULTS

#### Database

The benchmark NIST SD-4 database<sup>[26]</sup> was used to test the performance of the proposed classification algorithm. This database contains 4000 scanned fingerprint images from rolled impressions with a resolution of 500 dpi and of size  $512 \times 512$ . There are two impressions each of 2000 individuals labeled as F and S, for the first and second impressions, respectively. Each class (R,L,A,T,W) consists of 400 fingerprints. Class labels are assigned to each fingerprint in the database. There are 17.5% (350) ambiguous fingerprints with two class labels. The classification experiments are performed on this database using two protocols: one with the traditional approach used by many researchers in the literature and the other with the machine learning approach as described in the following two subsections 5.2 and 5.3, respectively.

### Evaluation Protocol-1

In this protocol, the NIST SD-4 database is partitioned into fixed training and testing sets. The training set (2000 fingerprints) is formed from the first and second impressions of the first 1000 fingerprints (F0001-F1000 and S0001-S1000) and the test set is formed from the remaining 2000 fingerprints (F1001- F2000 and S1001-S2000). For ambiguous fingerprints, only the first class label is used in the training set, while both class labels are used in the test set, a strategy used by almost all the researchers<sup>[10,13]</sup> in the literature. It prompted us to adopt protocol-1 to compare our results with previous approaches.

### Evaluation Protocol-2

In protocol-1, firstly, the predefined partitions of the database are used for training and testing, so the results obtained can depend on the chosen partition. Secondly, both the labels of ambiguous fingerprints are used for testing, making classification easy. Hence, as per the given guidelines,<sup>[16]</sup> we have used another protocol for a fairer comparison with the various fingerprint classification approaches. In this protocol, all the ambiguous fingerprints are removed (350 fingerprints with 2-class labels), and hence the new dataset is composed of 1650 fingerprints of each impression (F- and S-database) with a total of 3300 images. Instead of dividing the database into fixed training and testing set like the one used in protocol-1, which is followed by most of the previous researchers, which can ease the classification and may give optimal results, we have used a 5-fold Stratified Cross-Validation (SCV) procedure suggested by Galar *et al.*<sup>[16]</sup> Both the databases (F and S) are split into 5 folds, and at a time, one fold is used as a testing set and the remaining 4 folds as a training set this approach can provide a complete comparison from the perspective of the machine learning. The overall accuracy is calculated by averaging the five runs of the cross-validation.

### Fingerprint Quality and Rejection

The quality of fingerprints has a significant impact on fingerprint classification and fingerprint matching accuracy. Most AFIS, fingerprint quality checking is an essential step and is performed during the fingerprint enrollment phase itself. We have determined the quality level distribution using NIST Fingerprint Image Quality (NFIQ).<sup>[27]</sup> NFIQ gives five quality levels ranging from 1 to 5, 1 indicating the best and 5 indicating the worst quality. The NFIQ quality (1 to 5) distribution of NIST SD-4 database is 32%, 14.5%, 41.25%,

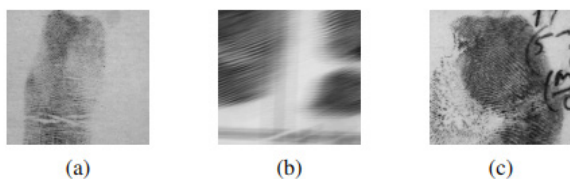


**Figure 6:** Examples of worst quality fingerprints (NFIQ=5) in NIST SD-4: (a) F0194, (b) F1192, (c) S1523

10.07% and 2.17% respectively. To avoid the effect of poor quality fingerprints on classification performance, we rejected a total of 104 (2.6%) fingerprints which includes 2.17% worst quality fingerprints, as shown in Figure 6, and the 0.42% fingerprints with registration points located at corners of images. The most important differentiable information of a fingerprint is located in the central region of the fingerprint, and hence the registration point's location in the center of the image is important for classification. Out of the total 4000 fingerprint images, only 0.42% of them are rejected due to the detection of registration points located near the image corners using the R92<sup>[21]</sup> algorithm. Finally, the 3896 fingerprints are used for fingerprint classification analysis using protocol-1 and protocol-2. Hence, we have used 1950 fingerprints for training and 1946 fingerprints for testing under protocol-1. In the case of protocol-2, the F and S databases consist of 1626 (1.45%) and 1605 (2.72%) fingerprints respectively. We have also evaluated the performance of the proposed algorithm over complete database and accuracy results are reported with and without rejection in Table 5 and 6 under protocols 1 and 2, respectively.

### Analysis of Scattering Parameters And Different Classifiers

The performance of the generative PCA affine classifier is compared with three other (SVM, k-NN, and ANN) discriminative classifiers. The most common classification rate metric is used for the performance analysis of these classifiers. It is defined as the ratio of the number of correctly classified fingerprints to the total number of fingerprints in the testing set. For SVM-based classification, LibSVM<sup>[32]</sup> was used to train a support vector classifier with an RBF kernel with regularity constant  $\gamma = 10^{-4}$  and all other hyperparameters kept at default values. For k-NN classification, Euclidean distance was used to find the k nearest neighbors with  $k = 5$  and  $k = 10$ . The neural network has an input layer size equal to the feature vector size, a hidden layer size of 1650, and an output layer size equal to the number of classes. It uses a binary cross-entropy loss function and a sigmoid activation function.

Table 1 shows the 5-class accuracy obtained using these three classifiers using protocol-1. To analyze the effect of scattering parameters on the classification performance, experiments with different values of scale (J), orientations (L), and scattering order (m) were conducted. We have kept  $J = 3$ ,  $L = 8$  and  $m = 2$  as the fixed parameters. The effect of each parameter is analyzed by varying the values of m, L, and J individually and is summarized in Table 2, Table 3 and Table 4, respectively. The first order ( $m = 1$ ) scattering coefficients are SIFT (Scale Invariant Feature Transform)-like features.<sup>[33]</sup> The SIFT method uses a Gaussian pyramid for a keypoint detection in an image by computing a local maximum on a

**Table 1:** Performance comparison of various classifiers

Classifier	SVM	5-NN	10-NN	ANN	PCA
Accuracy (%)	84.79	90.32	90.94	89.91	91.87



scale-space generated by isotropic Gaussian differences. It computes histograms of image gradient amplitudes around each keypoint. The second-order scattering coefficients capture the maximum high-frequency information,<sup>[20]</sup> which is useful for our classification problem. They carry sufficient discriminative information hence increasing  $m$  does not give much improvement. It can be noted that  $L = 8$  is adequate to capture directional information in the fingerprint. We used  $J = 3$  because using higher scales does not give any further advantage, as shown in Table 6.

**Table 2:** Effect of varying  $m$  with fixed  $J=3$  and  $L=8$

Order ( $m$ )	$m=1$	$m=2$	$m=3$
Accuracy (%)	24.19	91.87	91.25

**Table 3:** Effect of varying  $L$  with fixed  $J=3$  and  $m=2$

Orientations ( $L$ )	$L=4$	$L=8$	$L=12$	$L=16$
Accuracy (%)	89.65	91.87	90.22	91.46

**Table 4:** Effect of varying  $J$  with fixed  $L=8$  and  $m=2$

Scales ( $J$ )	$J=1$	$J=2$	$J=3$	$J=4$
Accuracy (%)	73.46	89.23	91.87	91.97

## Performance Comparison And Discussion

For a fair comparison, we compare the results reported by other researchers using two different protocols together with the result of our proposed approach on the benchmark database NIST SD-4. In Table 5, the results are compared using protocol-1, and Table 6 gives a comparative analysis using protocol-2. In addition to the classification rate, for protocol-2, Cohen's kappa<sup>[16,34]</sup> is used to evaluate the performance of the classification approaches. The difference between Cohen's kappa and classification rate lies in determining the score of the correct classifications. Classification rate scores all the successes based on all classes, while Cohen's kappa scores the successes classwise and finally aggregates all. The kappa is less sensitive to randomness due to varying samples in each class. This is mainly useful in protocol-2 due to the uneven distribution of samples in the F-database and S-database after removing 350 fingerprints with 2-class labels from 2000 fingerprints. The uneven distribution of remaining 1650 fingerprints is as: A = 380, L = 378, R = 373, T = 123 and W = 396. The kappa is computed using the confusion matrix (C) as:

$$kappa = \frac{N \times trace(C) - \sum_{i=1}^n S_{ci} S_{ri}}{N^2 - \sum_{i=1}^n S_{ci} S_{ri}} \quad (7)$$

**Table 5:** Comparison of various fingerprint classification algorithms using Evaluation Protocol-1 on NIST SD-4 database <sup>a</sup>.

Algorithms	Features	Classifier	5 – Class	4 – Class	Comments
Hong <i>et al.</i> [13]	GF, SP and RF	SVM and NB	90.8	94.9	Hybrid classification with multiple features and classifiers
Jain and Prabhakar [10]	GF	k-NN and ANN	90.4	94.8	Hybrid multichannel classifier using k-NN and neural network
Zang and Yan [5]	SP and RF	Rule-based	84.3	92.7	Incorporated a pseudo-ridge tracing along with singular points
Candela <i>et al.</i> [9]	OF	ANN	—	88.6	A combination of main (Probabilistic Neural Net) and auxiliary classifier (pseudo ridge tracer) is used.
Cappelli <i>et al.</i> [28]	OF	MKL and SPD	95.2	96.2	Uses a 2-stage (1 MKL based and 10 two-class SPD based classifiers) hybrid classification.
Liu [29]	SP	AbDT	94.1	95.7	Multiscale singularities features and Ad-boosted decision trees.
Karu and Jain [30]	SP	Rule-based	85.4	91.1	SP-based fixed rule classification.
Li <i>et al</i> [12]	OF and SP	SVM	93.5	95	Nonlinear OF phase portrait model and SP given to SVM.
Wang and Dai [6]	OF and SP	Rule-based	88.6	—	A novel singular point called core-delta is used.
Proposed (With Rejection*)	SWC	PCA affine	91.87	97.09	
Proposed (Without rejection)	SWC	PCA affine	88.76	94.31	Simple linear generative PCA classifier with deformation invariant

\* Rejection of 2.6% bad quality fingerprint images from NIST SD-4 Database under Evaluation Protocol-1 as discussed in section 5.4

**Table 6:** Comparison of various fingerprint classification algorithms using Protocol-2 on NIST SD-4 F and S databases.<sup>b</sup>

Algorithms	Features	No. of Features	Classifier	F-database		S-database	
				Accuracy	Kappa	Accuracy	Kappa
Hong <i>et al.</i> [13]	GF, SP and RF	202 (192 + 10)	SVM	89.49	0.8655	86.83	0.8299
Jain and Prabhakar [10]	GF	192	5-NN	88.38	0.8500	86.28	0.8233
Zang and Yan [5]	SP and RF	-	Rule based	87.63	0.8404	84.39	0.7988
Candela <i>et al.</i> [9]	OF	128	SVM	86.61	0.8283	85.45	0.8136
Cappelli <i>et al.</i> [31]	OF	357 (5 + 352)	SVM	87.45	0.8388	87.03	0.8337
Liu [29]	SP	64 (16 . 4)	5-NN	84.97	0.8061	82.73	0.7771
Karu and Jain [30]	SP	-	Rule based	84.55	0.8404	82.73	0.7771
Li <i>et al</i> [12]	OF and SP	58 (54 + 4)	SVM	73.27	0.6554	70.12	0.6143
Wang and Dai [6]	OF and SP	-	Rule based	75.56	0.6862	72.07	0.6409
Proposed (With Rejection*)	SWC	2604	PCA Affine	88.05	0.8689	86.97	0.8599
Proposed (Without Rejection)	SWC	2604	PCA Affine	87.48	0.8536	85.77	0.8481

<sup>a, b</sup> GF:Gabor filter response; SP:singular points; RF:Ridge line flow; OF:Orientation field; SWC:Scattering Wavelet Coefficients; NB:naiveBayes; ANN:Artificial neural network; SVM:Support vector machine ; k-NN:k-nearest neighbor; PCA:Principal component analysis;MKL:Multi-space KL; AbDT: Adaboosted decision trees; SPD:subspace pattern discrimination. \* Rejection of 1.45% and 2.72% bad quality fingerprint images from NIST SD-4 F-Database and S-Database respectively under Evaluation Protocol-2 as discussed in section 5.4.

where N = size of the test-set, n = number of classes, and Sri, Sci are row-sums and column-sums of C respectively, kappa lies between -1 and 1, where 1 indicates perfect classification. Many of the reported algorithms on fingerprint classification are based on the level-1 (SP and OF) features. Under rule-based classification,<sup>[2,29,30]</sup> the relative position and number of core-delta points are used. In addition, pseudo bridges are used along with SP to improve overall classification performance.<sup>[5]</sup> The orientation field (OF) is another dominant feature<sup>[6,8,9,12,28]</sup> used together with SP and ridgeflow information. This work mainly addresses the use of translation and small deformation invariant texture features using ScatNet to perform fingerprint classification. Compared with the methods discussed above, our approach has the following important features:

- The use of translation and small deformation invariant features to perform fingerprint classification by effectively utilizing the scattering wavelet network.
- The fingerprint ScatNet features are robust to noise and especially useful in live-scan acquisition to handle non-uniform pressure.
- A simple generative PCA affine classifier is used instead of other discriminative ones used by most researchers.
- Performance (classification accuracy and kappa) of the proposed approach is consistent under both protocols. It is proven<sup>[20]</sup> that scattering representation is stable to small deformations and additive noise while preserving the signal energy. The details about the properties of scattering wavelet transform and the related mathematical proofs can

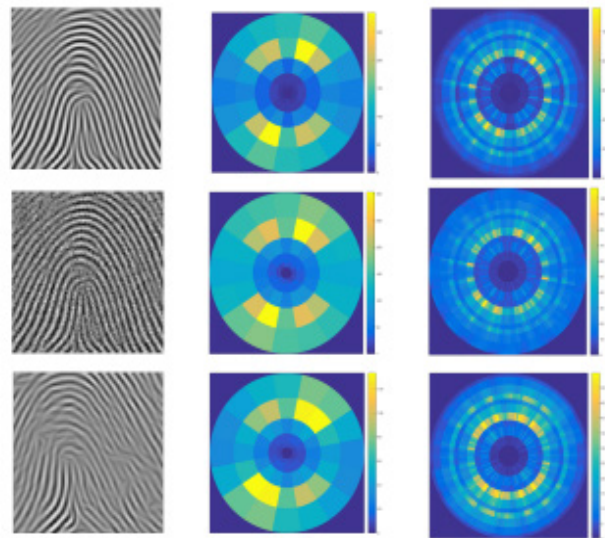


**Fig.7:** The scattering wavelet coefficient representation. From left to right: the original image, scattering coefficients of order  $m = 1$  and scattering coefficients of order  $m = 2$ . The top image corresponds to a normal fingerprint, the middle image is generated by adding Gaussian noise (variance = 0.04) and the bottom image is a deformed version of the top image

be found.<sup>[22]</sup> Figure 7 illustrates a polar representation of scattering wavelet coefficients introduced by Bruna *et al.*<sup>[20]</sup> and have been obtained by using the Matlab toolbox.<sup>[35]</sup> The



circular disk diagram is partitioned into different frequency sectors according to its radial axis and radius, depending on wavelet orientation ( $L = 8$ ) and scale ( $J = 5$ ) respectively. The scattering representation of the noisy and deformed images is not much different from the original image, which is necessary for classification application because images from intra-classes belong to a smooth manifold. Therefore, its representation must vary smoothly, as shown in Figure 7. Due to the unavailability of singular points in live-scan

Images, a few researchers<sup>[10,13]</sup> proposed Gabor filter-based features (eg: FingerCode<sup>[10]</sup>) which gave better results for fingerprint classification.

In the literature, the effect of deformation occurring due to non-uniform pressure applied during acquisition has not been addressed in the fingerprint classification problem. This work adopted a block-based approach to linearize the global deformation to an extent and then extracted scattering features for each block to build a complete local invariant model. This is the first paper to use deformation invariant features for fingerprint classification to the best of our knowledge. Detailed comparative performance analysis of the proposed algorithm is summarized

in Table 5 under protocol-1. The results reported in Table 6 are as per protocol-2. The protocol-2 is inspired by the work of Galar *et al.*<sup>[16]</sup> in which the previous algorithms are implemented by Galar *et al.*<sup>[16]</sup> under a common experimental framework to provide the baseline for future research work on fingerprint classification. The implemented results are given in Table 9 and Table 10 of Galar *et al.*<sup>[16]</sup> for F- and S-database, respectively. For protocol-2, the performance of the proposed approach is compared with the best performance (accuracy and kappa numbers highlighted with boldface in Table 9 and Table 10).<sup>[16]</sup> The composition number of features of the previous approaches, reported by Galar *et al.*<sup>[16]</sup> as given in Table 6. In the case of rule-based classification (number and position of core and delta), a feature vector is not mentioned (“-”) because no classifier training is required. Many algorithms use multiple features to improve classification accuracy. In such cases, the composition number is mentioned accordingly.

## Computational Complexity

The proposed algorithm consists of four main stages namely: registration point detection,<sup>[21]</sup> fingerprint enhancement,<sup>[25]</sup> ROI/ScatNet feature extraction and PCA affine classification. The registration point detection is implemented in C, while other stages are implemented in Matlab (2015a). The experiments over NIST SD-4 are conducted on a system with an Intel(R) Core-i7 (3.4 GHz) processor under the Windows 10 (64 bit) professional operating system having 8 GB RAM.

The average time required for these processing stages is 0.41, 2.47, 2.71, and 0.0047 seconds respectively. This classification time can be further reduced with C/Java implementation. Most of the computation time is used to extract the ScatNet feature. For an image of size  $N \times N$ , scattering transform yields a total of  $N^2 2^{-2j} \sum_{p=0}^m L^p \binom{L}{p}$  coefficients [20] and

with FFT implementation, the computational complexity is  $O(N \log N)$ . For real-time applications, special-purpose hardware like GPU (Graphics Processing Unit) along with a parallel computing platform like CUDA can decrease the overall processing time.

## CONCLUSIONS

This paper proposes a novel fingerprint classification algorithm that uses ScatNet to extract translation and small deformation invariant features. The extracted features are robust - they give a good classification accuracy with SVM, kNN, neural network, and PCA-based classifiers, as shown in Table 3. We use a simple generative PCA affine classifier which works best with the scattering features. The effect of various parameters of the scattering network has been analyzed, and it can be seen that the 2nd layer captures maximum discriminative information. Since the quality of fingerprints has a significant impact on fingerprint classification and minutiae feature extraction for matching, we have performed the quality checking by using the standard NIST-NFIQ algorithm<sup>[27]</sup> and 104 worst quality fingerprints are rejected. We achieved a classification accuracy of 91.87% (five-class) and 97.09% (four-class) under protocol-1 on the standard NIST SD-4 database. Some of the algorithms<sup>[6,12]</sup> which perform well under protocol-1 have failed to do so under protocol-2. But the proposed algorithm performs remarkably well under protocol-2 with an accuracy of 88.05% and 86.97% on the F and S databases, respectively. We have also evaluated the performance of the proposed algorithm without rejection and achieved a classification accuracy of 88.76% (five-class) and 94.31% (four-class) under protocol-1. An accuracy of 87.48% (F-database) and 85.77% (S-database) is achieved under protocol-2.

## ACKNOWLEDGMENTS

This work was supported by the National Center of Excellence in Technology for Internal Security (NCETIS) and the “Knowledge Incubation under TEQIP” initiative of the MHRD at IIT Bombay. We also wish to acknowledge the active participation of Shri. Brijesh Singh, Shri. Balsing Rajput, Shri. Prasad Joshi, and Shri. Deepak Dhole of the Department of Cyber Maharashtra, Mumbai.

## REFERENCES

- [1] A. Lumini, *et al.*, Continuous vs exclusive classification for fingerprint retrieval, *Pattern Recognition* 18 (10) (2010) 1027–1034.
- [2] M. Kawagoe, A.Tojo, Fingerprint pattern classification, *Pattern Recognition* 17 (3) (1984) 295–303.
- [3] E.Henry, *classification and uses of fingerprints*, Routledge, London,1900.
- [4] D. Maltoni, D. Maio, A. Jain, *Handbook of Fingerprint Recognition*, 2nd Edition, Springer-Verlag, New York Inc, 2009.
- [5] Zhang, Yan, Fingerprint classification based on extraction and analysis of singularities and pseudo ridges, *Pattern Recogn.* 37 (11) (2004) 233–243.

- [6] L. Wang, M. Dai, Application of a new type of singular points in fingerprint classification, *Pattern Recogn. Lett.* 28 (13) (2007) 1640–1650.
- [7] K. Rao, K. Balck, Type classification of fingerprints: A syntactic approach, *IEEE Trans. Pattern Anal. Mach. Intell.* 2 (3) (1980) 223–231.
- [8] R. Cappelli, *et al.*, Fingerprint classification by directional image partitioning, *IEEE Trans. Pattern Anal. Mach. Intell.* 21 (5) (1999) 402–421.
- [9] G. Candela, *et al.*, Pcasys-a pattern-level classification automation system for fingerprints, Tech. Rep. 5647, NIST (August 1995).
- [10] A. Jain, *et al.*, A multichannel approach to fingerprint classification, *IEEE Trans. Pattern Anal. Mach. Intell.* 21 (4) (1999) 348–359.
- [11] M. Pattichis, *et al.*, Fingerprint classification using an AM-FM model, *IEEE Trans. Image Process.* 10 (6) (2001) 951–954.
- [12] J. Li, *et al.*, Combining singular points and orientation image information for fingerprint classification, *Pattern Recognition* 41 (1) (2008) 353–366.
- [13] J. H. Hong, *et al.*, Fingerprint classification using one-vs-all support vector machines dynamically ordered with naïve Bayes classifiers, *Pattern Recognition* 41 (2) (2008) 662–671.
- [14] K. Cao, *et al.*, Fingerprint classification by a hierarchical classifier, *Pattern Recognition* 46 (2013) 3186–3197.
- [15] M. Galar, *et al.*, A survey of fingerprint classification part I: Taxonomies on feature extraction methods and learning models, *KB-Systems* 81 (2015a) 76–97.
- [16] M. Galar, *et al.*, A survey of fingerprint classification part II: Experimental analysis and ensemble proposal, *KB-Systems* 81 (2015b) 98–116.
- [17] R. Wang, *et al.*, A novel fingerprint classification method based on deep learning, in: *Conf. on Pattern Recognit, Cancun*, 2016, pp. 931–936.
- [18] W. Jeon, S. Rhee, Fingerprint pattern classification using convolution neural network, *International Journal of Fuzzy Logic and Intelligent Systems* 17 (3) (2017) 170–176.
- [19] D. Peralta, *et al.*, On the use of convolutional neural networks for robust classification of multiple fingerprint captures, arXiv preprint arXiv:1703.07270 [cs.CV] (2017).
- [20] J. Bruna, S. Mallat, Invariant scattering convolution networks, *IEEE Trans. Pattern Anal. Mach. Intell.* 35 (8) (2013) 1872–1886.
- [21] J. Wegstein, An automated fingerprint identification system, NBS Special Publication 500-89 (1982).
- [22] S. Mallat, Group invariant scattering, *Communications in Pure and Applied Mathematics* 65 (10) (2012) 1331–1398.
- [23] S. Laurent, S. Mallat, Rotation, scaling and deformation invariant scattering for texture discrimination, in: *Proc. of CVPR*, 2013, pp. 1233–1240.
- [24] <https://www.nist.gov/services-resources/software/nist-biometric-image-software-nbis>.
- [25] L. Hong, *et al.*, Fingerprint image enhancement: algorithm and performance evaluation, *IEEE Trans. Pattern Anal. Mach. Intell.* 20 (8) (1998).
- [26] C. Watson, C.L.Wilson, NIST special database 4, fingerprint database, Tech. rep., National Institute of Standards and Technology (1992).
- [27] C. Tabassi, *et al.*, Fingerprint image quality, Tech. rep., NIST (2004).
- [28] R. Cappelli, *et al.*, A two-stage fingerprint classification system, in: *Proc. of the 2003 ACM SIGMM WBMA*, 2003, pp. 95–99.
- [29] M. Liu, Fingerprint classification based on adaboost learning from singularity features, *Pattern Recognition* 43 (3) (2010) 1062–1070.
- [30] K. Karu, A. Jain, Fingerprint classification, *Pattern Recognition* 29 (3) (1996) 389–404.
- [31] R. Cappelli, *et al.*, A multi-classifier approach to fingerprint classification, *Pattern Anal. Appl.* 5 (2002) 136–144.
- [32] C. Chang, C. Lin, LIBSVM: A library for support vector machine, *ACM Trans. Intell. Syst. Technol.* 2 (2011) 27:1–27:27.
- [33] D. Lowe, Distinctive image features from scale-invariant keypoints, *International Journal of Computer Vision.* 60 (2) (2004) 91–110.
- [34] J. Cohen, A coefficient of agreement for nominal scales, *Educ. Psychol. Measure.* 20 (1) (1960) 37–46.
- [35] <http://www.di.ens.fr/data/software/>
- [36] Parmeshwar Birajadar *et al.*, Unconstrained Ear Recognition Using Deep Scattering Wavelet Network, 2019 IEEE Bombay Section Signature Conference (IBSSC), 2019.

